Andreas B. Dahlin[a], Nathan J. Wittenberg[a], Fredrik Höök and Sang-Hyun Oh*

Promises and challenges of nanoplasmonic devices for refractometric biosensing

Abstract: Optical biosensors based on surface plasmon resonance (SPR) in metallic thin films are currently standard tools for measuring molecular binding kinetics and affinities – an important task for biophysical studies and pharmaceutical development. Motivated by recent progress in the design and fabrication of metallic nanostructures, such as nanoparticles or nanoholes of various shapes, researchers have been pursuing a new generation of biosensors harnessing tailored plasmonic effects in these engineered nanostructures. Nanoplasmonic devices, while demanding nanofabrication, offer tunability with respect to sensor dimension and physical properties, thereby enabling novel biological interfacing opportunities and extreme miniaturization. Here we provide an integrated overview of refractometric biosensing with nanoplasmonic devices and highlight some recent examples of nanoplasmonic sensors capable of unique functions that are difficult to accomplish with conventional SPR. For example, since the local field strength and spatial distribution can be readily tuned by varying the shape and arrangement of nanostructures, biomolecular interactions can be controlled to occur in regions of high field strength. This may improve signal-to-noise and also enable sensing a small number of molecules. Furthermore, the nanoscale plasmonic sensor elements may, in combination with nanofabrication and materials-selective surface-modifications, make it possible to merge affinity biosensing with nanofluidic liquid handling.

Keywords: Optical biosensors; refractometric sensors; surface plasmon resonance; plasmonics; figure of merit; single molecule detection; enzyme-linked biosensing; site-specific chemistry; supported lipid bilayer; pore-spanning lipid membrane; nanoparticle; nanohole; optofluidics.

[a]These authors contributed equally to this work.
*Corresponding author: Sang-Hyun Oh, Laboratory of Nanostructures and Biosensing, Department of Electrical and Computer Engineering, University of Minnesota, Twin Cities, 200 Union St. S.E., Minneapolis, MN 55455, USA, e-mail: sang@umn.edu
Sang-Hyun Oh: Department of Biophysics and Chemical Biology, Seoul National University, Seoul 151-747, Korea
Andreas B. Dahlin and Fredrik Höök: Division of Bionanophotonics, Department of Applied Physics, Chalmers University of Technology, Fysikgränd 3, 41296, Göteborg, Sweden

Nathan J. Wittenberg: Laboratory of Nanostructures and Biosensing, Department of Electrical and Computer Engineering, University of Minnesota, Twin Cities, 200 Union St. S.E., Minneapolis, MN 55455, USA

1 Introduction

Optical imaging, sensing, and trapping instruments have been among essential tools for life sciences and biotechnology, as illustrated in the examples of laser confocal scanning microscopy, fluorescence-activated cell sorters, optical tweezers, and surface plasmon resonance (SPR). With the completion of the Human Genome Project, there is a tremendous demand to catalogue proteins and to map their complex networks of interactions with other proteins, lipids, carbohydrates, nucleic acids, and drug molecules in a quantitative manner. SPR instruments are surface-based optical biosensors that can measure the kinetics and affinities of these diverse biological interactions in real-time by monitoring the interfacial refractive index changes caused by molecular interactions without having to label the molecules. Over the past two decades, SPR has become the "gold standard" in quantifying molecular binding kinetics – a task that is becoming increasingly important in the field of proteomics, systems biology, and drug discovery – and there is an increasing demand to improve its sensitivity, functionality, throughput and the information content in the measured response.

This review article will discuss how the emerging field of nanoplasmonics may further improve this unique and commercially important sensing technology. Focus is put on real-time measurements utilizing refractometric detection [1], i.e., changes in the far-field optical properties induced by the local change in refractive index (RI) on the surface upon molecular binding. The ultimate goal of SPR sensing is real-time measurements of binding kinetics between molecules. It should be emphasized that the overall sensor performance is determined not only by the sensitivity of the plasmonic nanostructure, but also depends heavily on the biorecognition elements employed. Therefore, rather than narrowly focusing on the physics of nanoplasmonic

sensors, this review will provide an integrated view on refractometric SPR biosensing technologies, including plasmon resonances in nanostructures, biorecognition elements and surface modification strategies, mass transport effects, optical instrumentation and noise reduction techniques, and various performance metrics. Some emphasis will also be given to techniques for systems designed to interface biology. Our goal is to compare conventional SPR instruments with emerging nanoplasmonic sensors, in particular localized surface plasmon resonance (LSPR) and nanohole sensors based on the extraordinary optical transmission (EOT) effect. Finally, we show some recent highlights in using nanoplasmonics to demonstrate sensing tasks that are not easy or impossible to perform using conventional SPR.

2 Plasmonic nanostructures

With the main focus of this review being recent advantages within nanoplasmonic biosensing, we will here give a shortened overview of the history, physics and biosensor applications of plasmon resonances in nanostructures. Appropriate references, especially to review articles and books, are provided for further reading. We also give a brief discussion on how the sensitivity of a given nanostructure is (or should be) evaluated.

2.1 Nanoparticle plasmons

The bright colors of noble metal nanoparticles have been utilized historically for decorative purposes e.g., in glass [2] and on ceramics [3]. In addition, colloidal gold has long been associated with various health benefits [4] and is now beginning to appear in more sensible applications in modern medicine [5].

The quantitative physical description of the localized plasmons in gold nanoparticles was presented by Mie slightly over 100 years ago [7]. An extension from spherical to spheroidal particles was given shortly after [8]. Although these theories are complete analytical solutions to Maxwell's equations (for homogenous isotropic materials), it is common to present simplified equations based on electrostatics [9]. For an arbitrary ellipsoid, the polarizability is then [10]:

$$\alpha_0 = V \frac{\varepsilon(\omega) - n^2}{n^2 + L(R_1, R_2, R_3)\left[\varepsilon(\omega) - n^2\right]} \quad (1)$$

Here $V = 4\pi R_1 R_2 R_3 / 3$ is the ellipsoid volume, $\varepsilon(\omega)$ is the complex dielectric function of the metal (dispersive by

dependence of angular frequency ω) and n is the refractive index (RI) of the environment. The far field extinction and scattering cross sections are acquired from $\sigma_{ext} = k\ \text{Im}(\alpha)$ and $\sigma_{sca} = k^4 |\alpha|^2 / [6\pi]$ [11], where $k = 2\pi n / \lambda$ is the wavevector (λ is the vacuum wavelength). Notably, the scattering scales with the square of volume V and absorption of light is the primary decay mechanism in smaller particles (tens of nm). The parameter $L(R_1, R_2, R_3)$ in Eq. (1) is the shape-determined factor associated with a given ellipsoidal axis, so that each axis has its own dipolar resonance [11]. (Each L ranges from zero to one and $L_1 + L_2 + L_3 = 1$.) Eq. (1) fails to describe particles that are comparable in size to the wavelength of light (typically >50 nm) due to retardation, higher order modes and radiative damping [9]. However, analytical approximations are available that describe the dipolar resonance contribution to the spectrum. The most commonly used is the modified long wavelength approximation, which defines a more accurate polarizability as a function of the quasistatic polarizability: [12, 13].

$$\alpha = \frac{\alpha_0}{1 - i\dfrac{k^3}{6\pi}\alpha_0 - \dfrac{k^2}{4\pi R_j}\alpha_0} \quad (2)$$

Here R_j is the radius of the ellipsoid dipole axis. Eq. (2) gives excellent agreement with experimental data, even in absolute extinction magnitude, when used to model the spectrum of e.g., nanodisks [14] (oblate spheroids). Further, there are analytical models that take into account the presence of a shell coating [11], which is particularly interesting for modeling the spectral changes induced by molecular binding in biosensing experiments. Also, the presence of a solid support, which is often included in biosensing applications, can be accounted for [15] simply by modifying the value of L and making it depend on the RI of the solid support [16].

Most plasmonic biosensors based on nanoparticles utilize spheres [17–20], rods [21–23], disks [24] or shells [25] and can thus be modeled analytically as described above. However, when dealing with particle shapes that deviate too much from ellipsoids, such as triangles [26], rings [27], octahedrons [28] or "stars" [29], one is forced to use numerical approaches. This is also the case for more complex nanostructures containing particles in close proximity, in which case the individual resonances hybridize and produce new modes. There has been a recent interest in so-called Fano resonances appearing in such structures [30], not the least for refractometric sensing [31] (Figure 1).

In the beginning of the 1900s, colloidal gold was used for diagnostics of cerebrospinal fluid [32, 33]. The first refractometric biosensing experiments with suspended
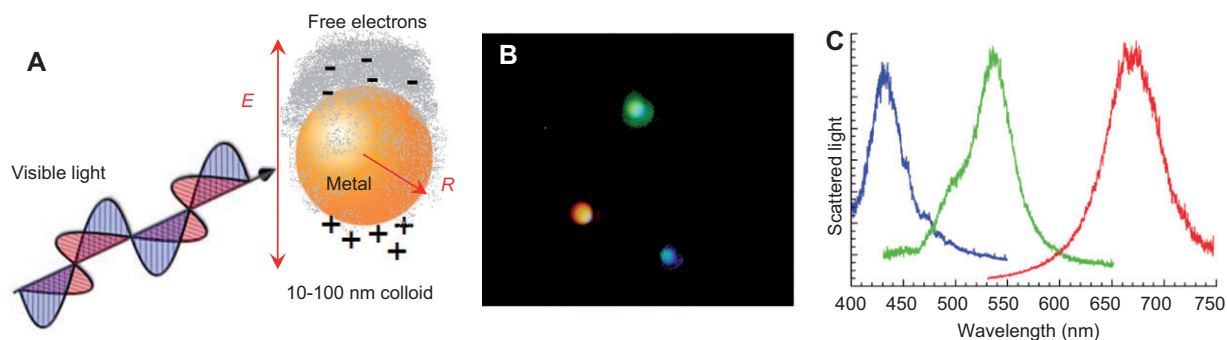
Figure 1 (A) Metallic nanoparticles can support localized surface plasmon resonance (LSPR), collective oscillations of the conduction electrons excited by light. (B) A color photograph of single metallic nanoparticles illuminated with white light. (C) Scattered light spectra measured from nanoparticles shown in (B). Images (B) and (C) adapted from Schutz [6].

nanoparticles were reported by Englebienne et al. in 1998 [17]. One year earlier, Mirkin's group had showed the first assay based on plasmonic coupling between suspended nanoparticles [34]. In the following years, many papers appeared where various nanoparticles on surface supports were used for refractometric detection, e.g., from the groups of van Duyne [26] (triangular silver particles), Chilkoti [18] (immobilized colloidal gold), Höök [35] (quantification of LSPR response), and Rubinstein [36] (gold "islands").

2.2 Surface plasmons

The most important work for understanding the nature of surface plasmons is arguably what was presented in the middle of the 20th century by Ritchie [37], who used Maxwell's equations to show that an electromagnetic wave (with transverse magnetic polarization) can exist and be confined to an interface between a metal and a dielectric. The concept of surface plasmons was used to explain the appearance of additional resonances (besides the metal bulk plasma frequency) in electron energy loss spectroscopy of thin metal foils [38].

The fundamental difference between propagating surface plasmons and nanoparticle plasmons (often referred to as localized surface plasmons) is that they appear in a continuum of frequencies. Propagating surface waves carry a momentum and are described by a dispersion relation. For the simplest case with a single planar metal-dielectric interface (semi-infinite materials) one has [39]:

$$k_x = \frac{\omega}{c}\sqrt{\frac{\varepsilon(\omega)n^2}{\varepsilon(\omega)+n^2}} \qquad (3)$$

Here k_x is the (complex) in-plane wavevector of the surface plasmon and c is the speed of light in vacuum.

Excitation of surface plasmons by light requires matching both the frequency (energy) and wavevector (momentum) of incident photons, which is impossible under normal circumstances since the dispersions do not cross without additional photon momentum [40]. The k of incident photons is normally increased either utilizing total internal reflection and a thin metal film (Kretchmann configuration for SPR; Figure 2) or by a grating on the metal surface.

Importantly, since an optically thin film or a periodically patterned nanostructure is required for SPR, the dispersion relation in Eq. (3) is always merely an approximation. A more accurate calculation of the resonance condition requires that the dispersion is modified such that it accounts for the fact that the metal film is finite in thickness (prism coupling in total internal reflection) or that scattering occurs at the structured surface (grating coupling). A convenient way to calculate the full spectrum in reflection spectroscopy is by Fresnel calculations using the transfer matrix method [1].

The first utilization of surface plasmons in biosensing came in 1982 from Liedberg et al. [42] and today surface plasmon resonance (SPR) is the primary established (and commercialized) method for quantitative real-time analysis of biomolecular interactions, generating thousands of papers every year [43]. Lately, more sophisticated SPR sensors have been developed, based on phase detection [44, 45] or long-range surface plasmons [46, 47].

2.3 Nanohole arrays

The third of the most common type of nanostrucures used in plasmonic biosensors are nanoholes in thin metal films (Figure 3) [48–50]. Considering first the case of a single hole, one can use electrostatic theory
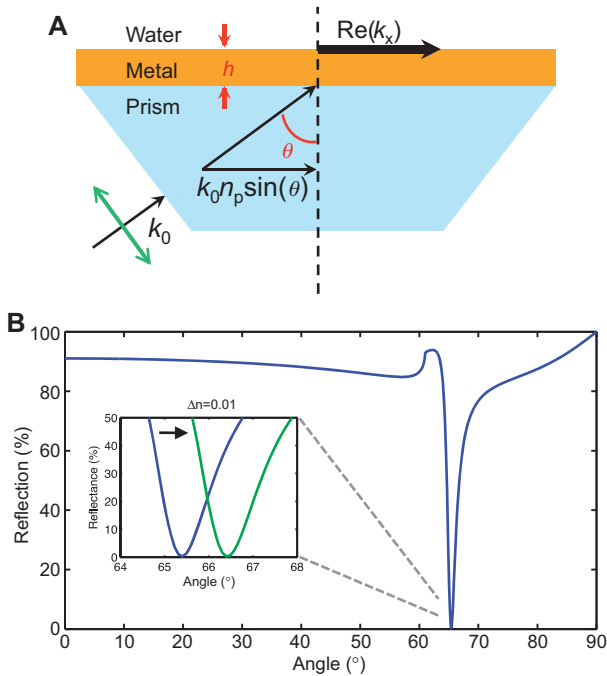
Figure 2 (A) A prism-coupler setup (also known as Kretschmann setup) for the excitation of SPR in thin metallic films. (B) Coupling to surface plasmons is detected by a sharp reduction in reflectance at a certain excitation angle. Shown here is the simulated reflection of a 50 nm-thick gold film on a glass substrate as a function of incident angle for 850 nm illumination. By changing the refractive index of the solution by Δn=0.01, the resonance (dip) shifts by 1° in this example, corresponding to the sensitivity of 100°/(refractive index unit). From Lindquist et al. [41].

to show that a void in a metal should have a resonant polarizability quite similar to a nanoparticle (Figure 3A) [10]. Further analogies between holes and particles were predicted already in 1954 by Bethe, who calculated the effective scattering cross section of a circular aperture in an infinitely thin perfect conductor [51]. There seems to be a general consensus that single holes exhibit localized resonances similar to nanoparticles, i.e., high sensitivity to shape changes and polarization [52]. The optical properties of *arrays* of nanoholes have been intensely studied since Ebbesen observed resonant transmission through square arrays in opaque gold and silver films [53].

In arrays of nanoholes (Figure 3B and D) one faces two principle types of resonances that couple to each other. One is the localized (particle-like) modes associated with individual holes and the other is surface plasmon excitation induced by the periodicity of holes in an array. Interestingly, short-range order in the arrays is sufficient for an SPR effect, i.e., structural correlation over longer distance (microns) is not necessary [54–56]. For the case of

coupling to surface plasmons at normal incidence using nanoholes, the resonance condition is simply:

$$\frac{2\pi}{\text{Re}(k_x)}j=P \qquad (4)$$

This expression simply illustrates that the periodicity P of the array should equal a multiple of the surface plasmon wavelength. For short-range ordered arrays, P is simply the characteristic spacing between holes [55]. The challenge lies in coming up with an accurate expression for the dispersion relation so that Eq. (4) actually can be used to predict the resonance. In particular, one must account for the fact that the metal now contains holes. This leads to a redshift in the measured resonance, which can be understood as an effectively reduced plasma frequency (electron density) of the metal upon perforation [55]. The situation is overall more complicated in optically thin films since they show significant "ordinary" transmission of light and strong hybridization between the surface plasmons at either interface [55, 57]. Also, a thin film prevents Fabry-Pérot type modes that propagate through individual holes (perpendicular to the surface).

Although there are well-known [58, 59] and extensive [60, 61] reviews on the optical properties of nanohole arrays, inconsistencies seem to remain in the literature still. For instance, in most work on >100 nm films the *transmission* maximum is associated with the surface plasmon, as originally suggested [53]. However, it is also known that this approach does *not* provide accurate predictions of the resonance wavelength. There are theories that can explain this offset [62], but it has also been shown that the predicted resonance for various arrays agrees well with an *extinction* maximum [56]. For the case of thinner films (10–50 nm) it seems quite clear that the extinction peak indeed corresponds to surface plasmon excitation [55, 63]. Even for single holes, some controversy on the optical properties remains since it has been suggested that they exhibit no localized resonances, but enable direct coupling to surface plasmons [57]. Although a detailed physical description of the optical properties of nanohole arrays is not critical in many sensing situations, it becomes important when attempts are made to quantify the response in terms of bound mass, in the analysis of binding kinetics or if the performance of the sensor must be improved.

The first reports on biosensing through RI changes with nanohole arrays appeared in the early 2000s. Brolo et al. utilized resonant transmission through long-range ordered arrays in thick (100 nm) Au films [64], while Dahlin et al. used short-range ordered nanoholes in thin
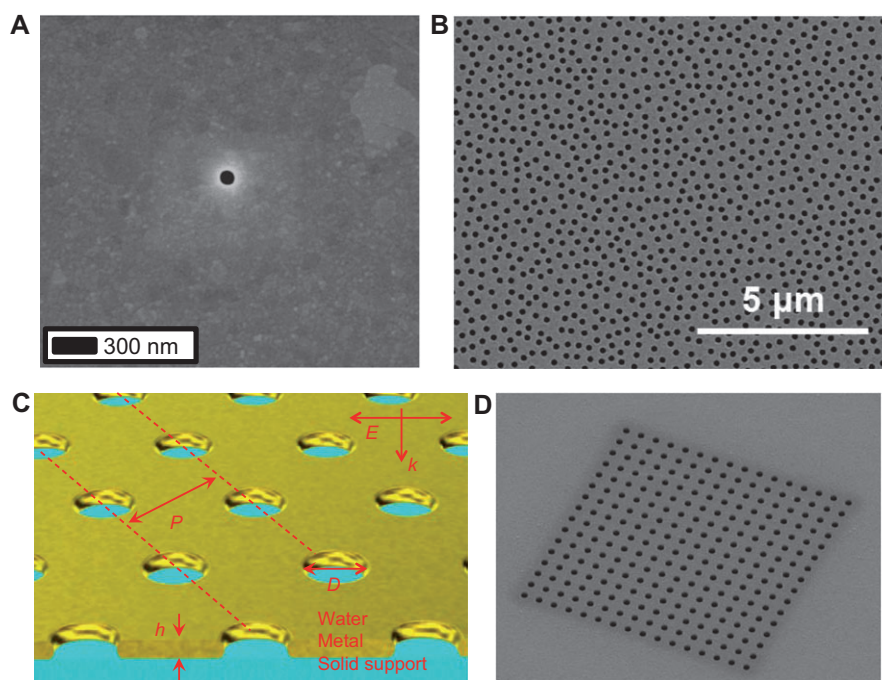
Figure 3 Metallic films perforated with nanoholes can support both propagating surface plasmons as well as LSPR-type resonances in the voids. (A) An isolated hole (100 nm in diameter) milled with FIB in a silver film. Image courtesy of Nathan Lindquist. (B) A random hole array in a metal film produced by colloidal lithography. (C) Schematic of periodic hole arrays in a metal film with a solid support. (D) A periodic array of nanoholes (200 nm diameter; 600 nm periodicity) milled with FIB in a gold film. Image courtesy of Hyungsoon Im.

(20 nm) Au films [65]. The Käll group presented the first biosensing experiments on single holes [66].

2.4 Sensitivity evaluation

How can one evaluate whether a plasmonic nanostructure, including a thin planar metal film for Kretschmann SPR, would be suitable for biosensing? This depends first of all on the transduction mechanism. For example, a sensor based on particle-particle coupling [67] needs to have the biorecognition event cause a relatively large change in the distance between the metal particles. We focus here on how to evaluate the sensitivity in terms of refractometric detection, i.e., signal generation caused by a change in interfacial refractive index induced by a biomolecular recognition reaction.

The research field of nanoplasmonic sensors emerged in synergy with advances in nanofabrication [41]. There was a great interest in testing new fabrication methods with the aim of finding "more sensitive" nanostructures, as exemplified above. This is still the case and now more sophisticated spectroscopy techniques such as phase detection are utilized as well [44, 68]. Naturally, one must consider carefully how the sensing capabilities should be evaluated, so that a sensor that has a higher "sensitivity" actually provides a better detection limit when employed for biomolecular sensing (although the actual resolution will, in the end, also depend on the instrumentation used for spectroscopy). Most early papers focused on the *resonance shift* per change in RI of the liquid environment. This is logical since our physical understanding of all refractometric plasmonic sensors is that the resonance shifts to lower energy (longer wavelength) when the RI of the environment is increased. Later, it became more common to use the "figure of merit (FOM)", which (usually) means the peak-shift sensitivity divided by the peak width. While the FOM serves as a convenient metric to evaluate the performance of refractometric sensors, this parameter alone may not accurately predict the detection limit for real biomolecular sensing. For example, while a prism-based Kretschmann SPR instrument has a broader linewidth than optimized nanoplasmonic sensors, it still has a better detection limit in terms of molecular surface coverage (commercial Biacore™ instruments can go down to 0.01 ng/cm^2) than nanoplasmonic sensors. With proper curve fitting algorithms and noise reduction schemes, a very small spectral shift (~0.001 nm) from a relatively broad SPR dip can be readily resolved [69]. In terms of surface coverage, this corresponds to ~0.1 ng/cm^2. On the

other hand, if a sharp peak is obtained at the expense of reduced peak intensity, the overall performance may actually degrade. A paper from the Masson group suggested that the *magnitude* of the peak should be taken into account [70]. For SPR kinetic measurements of rapid association or dissociation kinetics between molecules, one needs high temporal resolution and thus high photon flux, which also implies that the intensity of the peak or dip is of great importance. Rather than using the FOM defined above, one could argue that the minimum detectable RI change, or sensor resolution, may be a more realistic metric for SPR and nanoplasmonic sensors. Naturally, such a performance parameter also takes into account the quality of the optical components and the experimental setup (see below). However, a high resolution for bulk refractive index changes does not always translate into an improved detection limit for surface-bound molecules. For example, with a temperature control and mechanical stabilization, the resolution of prism-based SPR is approaching 10^{-7} refractive index units [71]. While LSPR sensors cannot match such high refractive index resolution, they could show relatively similar performance for detecting surface-bound molecules.

As illustrated here, the discussion on how to evaluate sensitivity continues. Dahlin has presented detailed discussions on the topic [1, 72], suggesting that the refractometric sensitivity is best defined in terms of relative intensity changes (e.g., extinction, transmission) per RI increase. In brief, the primary argument behind this conclusion is that a change in light intensity is the one and only thing that can be measured by a photodetector and thus it forms the basis for the sensor output. The same idea has been indicated in a few other papers that used a normalized intensity to evaluate the refractometric sensitivity [20, 73]. From this point of view, peaks that shift more, are narrow and *strong in magnitude* are preferable simply because they tend to give rise to higher intensity changes in the photodetector. Das et al. compared the signal-to-noise performance of different analysis methods for nanohole SPR sensors [74].

Regardless of which parameter is chosen to represent refractometric sensing performance, one must also consider the extension of the plasmonic field into the liquid environment. It is widely accepted that nanoplasmonic sensors, especially those utilizing LSPR, have a shorter field extension (tens of nm) compared to Kretschmann SPR (hundreds of nm), making them more suitable for surface constructs consisting of biomolecular monolayers [75]. However, in most SPR systems a 3D dextran matrix coating is used, which makes it possible to utilize the whole probing volume and enhance the signal [76].

A recent study showed that for gold nanoislands, the field extension scaled approximately linearly with the liquid bulk sensitivity in terms of resonance shift per RI change [77]. This suggests that as long as one works with biomolecular layers smaller than the field extension, the signal will be roughly the same regardless of the choice of nanoparticle.

3 Fabrication techniques for nanoplasmonic sensors

In contrast to Kretschmann SPR, which works with simple flat gold films, nanoplasmonic substrates must be produced via top-down nanofabrication or bottom-up synthesis to pattern holes, particles, slits, etc. Recent advances in fabrication and synthesis techniques for nanoplasmonic structures have resulted in improved throughput, shape control, reproducibility and optical properties. For example, earlier work on studying EOT effects mainly relied on focused ion beam (FIB) milling [53] to pattern periodic hole arrays typically at the scale of tens of microns, due to the low throughput of those serial writing techniques. While colloidal lithography has been used for large-area patterning of short-ranged ordered nanoholes [78], it is difficult, although possible, to make long-range periodic hole arrays [50, 79]. The growing interest in using metallic nanoholes for sensing and other applications has motivated researchers to develop practical routes to fabricate large-area (~mm to cm) periodic nanohole arrays, such as interference lithography [80–82], nanoimprint lithography, or template stripping [83–85]. Lindquist et al. summarized various top-down fabrication methods for making nanoplasmonic structures in a recent article [41].

The optical performance of nanoplasmonic devices depends on various factors such as surface roughness, crystallinity [14], morphology (grain size and grain boundaries), and dielectric functions of the metal itself. One key advantage of nanoparticle sensors made with colloidal synthesis is that they are single-crystalline in nature, which reduces plasmon damping due to electron scattering at grain boundaries. In contrast, metal films deposited by conventional evaporation or sputtering are polycrystalline, and thus exhibit roughness. Unfortunately, tightly confined SP waves are not only sensitive to surface-bound analytes, but also to unwanted surface roughness, grain boundaries, and surface contaminants. Indeed it was shown than reducing the roughness from ~5 nm to sub-1-nm in a Ag film increased the plasmon propagation length by 3–5× at visible wavelengths [83]. To minimize

surface roughness and improve the dielectric functions of metal films, groups have shown techniques such as template stripping and the growth of single-crystalline metal films [86].

4 Plasmon spectroscopy for high-resolution biosensing

4.1 Experimental setup

What are the pros and cons of nanoplasmonics compared to SPR in terms of simplicity when performing spectroscopy? When the research field of nanoplasmonics started up, it was commonly claimed that one advantage is the possibility to be able to perform simpler spectroscopy, in transmission mode instead of the Kretschmann configuration [36, 64]. This has some truth because "ordinary" spectrophotometers, found in practically every molecular biology lab, can then be used in the sensing experiments [20, 36, 64, 65]. In terms of components needed for the experimental setup, the Kretschmann SPR is no more complicated. Homola's group has presented simple and compact prism-based SPR sensors with high performance [87, 88]. However, performing transmission-mode spectroscopy (e.g., using nanohole arrays) in collinear setup offers some practical advantages, since it is more forgiving to a sample misalignment or tilt compared with the Kretschmann setup. Furthermore, as Tetz et al. pointed out [80], wide-field SPR imaging with a high-numerical-aperture (NA) lens, which is desirable to gather molecular binding kinetics from a dense microarray of sensing elements, is difficult to perform with the Kretschmann setup because of the limited depth of focus caused by the prism and oblique illumination. Wide-field, high-NA SPR imaging is considerably easier to perform with nanohole arrays [89], since it can operate with normal illumination and collection with high-NA imaging optics.

On the other hand, it should be noted that reflection-mode operation can also offer several advantages. Most notably, it simplifies measurements on opaque liquids and the top sensor surface is also freely accessible for integration with other analytical tools that may block optical paths in a transmission measurement setup. Recent work has now introduced reflection-mode measurements also for nanoplasmonic sensors [90–92]. Using template-stripping methods, backside reflection-mode nanoplasmonic sensor has also been demonstrated [92], wherein the optical paths and fluidic paths are decoupled as with conventional SPR.

In summary, a key advantage of the prism-based Kretschmann setup is the fact that there is no need for lithographic patterning (the metal structure is just a thin film), while its oblique illumination optics puts some restrictions on the optical system. Nanoplasmonic sensors put more burdens on the chip fabrication, but have potential to simplify optical systems design and allows one to tailor the location and width of plasmon resonance peaks by patterned geometries. These pros and cons should be considered when choosing nanoplasmonics vs. conventional SPR for a given application.

4.2 Noise minimization

We will here mention some simple methods for eliminating the most common types of noise in optical spectroscopy. In any sensor, the limit of detection is eventually determined by not only the sensitivity of the plasmonic nanostructure, but also the instrumentation used for reducing noise. Judging from the literature, relatively little effort is spent on noise reduction compared to chasing high sensitivity. Obviously, the experimental setup must be mechanically stable, especially when measuring on smaller samples [24, 93]. Temperature control is normally more important for SPR because of the high sensitivity to changes in the liquid bulk RI. For instance, the RI of water decreases with 8×10^{-5} per K (at room temperature), suggesting that the temperature needs to be controlled almost down to 0.01K to maintain instrumental resolution. Although spectral changes can be induced by temperature changes in the dielectric environment, the temperature of the *metal* may be even more important for stability [94] if it is strongly heated by the probing light [95]. Another possible reason for instability is the light source. Quite high resolution (surface coverage of 0.1 ng/cm^2) can be reached without the need of updating the reference spectrum [69], but continuous updates of the source intensity may be needed when pursuing even lower noise [44].

For a stable experimental setup in a reasonably well-controlled environment, one can expect that most of the noise originates from the photodetector. There are three types of false electrons generated in the detector that do not originate from photons that have interacted with the sensor. First, thermal electrons are always present, but their contribution can be greatly reduced by cooling the detector. Second, there are electrons generated in the readout process. If significant, this noise can be reduced by gain in the detector. Third, there can be background light

reaching the detector. (The solution is to work in the dark.) However, all these types of detector noise become insignificant if the probing intensity is high enough to dominate the photodetector response. It is then possible to reach the shot-noise limit, as can be verified by looking at the noise characteristics [24]. Since shot-noise is part of the nature of light it cannot be truly eliminated, but its contribution to the overall noise can be reduced, again by operating at high intensity and by using photodetectors with high dynamic range [69, 96].

4.3 Multiplexed operation

It is often preferable to screen multiple biomolecular interactions or detect the presence of several analytes in a sample simultaneously. A small degree of multiplexing with particles *in solution* can be achieved by measuring the spectrum of a mixture of nanorods with different aspect ratio [L in Eq. (1)], so that the spectral peaks are reasonably well separated [21]. However, normally multiplexing is achieved by operation in imaging mode on the surface, i.e., dispersive information is replaced with information on spatial intensity variations. If the full spectrum (not just one intensity value) needs to be acquired from several locations on the surface simultaneously, or from a linear array of parallel microfluidic channels, one can use 1D spectral imaging [97, 98]. Using some "tricks", it is also possible to acquire the full scattering spectrum of well-separated individual nanoparticles (on a 2D surface) in parallel [99]. For SPR, operation in imaging mode for multiplexing is an established technique [40] and does not necessarily result in loss in resolution [87]. Also for nanohole arrays [82, 89, 100–102] and dense nanoparticle samples [103], imaging operation for multiplexed biosensing has been introduced.

4.4 Scattering spectroscopy

When performing spectroscopy in transmission or reflection mode, the intensity reaching the photodetector consists of light which has *not* coupled to any plasmon. An alternative technique is to only detect light which originates from radiative decay of plasmons, i.e., scattering spectroscopy. This requires a dark background and the technique is well suited for imaging plasmonic nanoparticles. Establishing dark-field illumination is relatively straightforward, but often requires that a significant amount of the excitation light is blocked in order to avoid direct transmission to the collection optics. One way to avoid this loss in intensity is to utilize total internal reflection for generating the dark field [104]. Dahlin et al. have addressed the question in which situations scattering spectroscopy provides better signal to noise than operation in transmission mode [24], suggesting that scattering spectroscopy is preferable only when measuring on single nanoparticles.

5 Highlights in nanoplasmonic sensing

5.1 Single molecule resolution

One early major driving force for the development of nanoparticle-based LSPR sensors is the possibility to perform spectroscopy on single nanoparticles [19, 22, 23, 25, 29, 105], which clearly represents an extremely small (~50 nm or below) sensor that cannot be easily constructed using diffraction-limited dielectric components. In fact, even a sensor based on propagating surface plasmons would never enable this degree of miniaturization due to limitations on how well light can be focused and the propagation length of the plasmons (several μm). It was shown in relatively early papers that the signal to noise in real-time measurements on light scattering from single particles was *almost* sufficient for resolving single molecules (typically a protein) binding to the particle [22, 106]. Enzymatic precipitation has been used to amplify the response post-binding, and it was argued that such an assay could provide single molecule detection although not in real-time [107]. By enhancing the illumination intensity (white light laser in total internal reflection) and optimizing nanoparticle geometry, Sönnichsen's group recently reported resolving single relatively large protein molecules (fibronectin, 450 kDa) adsorbing on a gold nanorod [104].

The real-time detection of individual protein molecules binding to receptors on the nanoparticle surface, i.e., an operational biosensor, was recently shown by Zijlstra and coworkers [108]. Not surprisingly, this required a significantly more sophisticated spectroscopy technique based on photothermal microscopy [109]. In this method, two laser sources illuminate the nanoparticle. One beam is used for heating the nanoparticle (absorption, i.e., σ_{abs}) while the other beam is used as a probe for measuring the thermal signal. Upon biomolecular binding to the nanorod, the plasmon resonance shifts as usual (Figure 4A). However, instead of attempting to detect the resonance shift directly through scattering spectroscopy, the fact that the absorption (and thus the temperature) is

changed was utilized and single binding events could visualized in the thermal signal [108] (Figure 4B). As mentioned above, since absorption scales with the volume of the nanoparticle (while σ_{sca} scales with V^2), thermal microscopy enables the use of very small nanoparticles [109] (31×9 nm), which provide an extremely confined probing volume suitable for enhancing the response from a single molecule.

Although single-molecule resolution can be considered a highly impressive achievement by most standards, one should also ask the question in which sensing applications it would be relevant to see individual binding events. It is important to note that *all* molecules are not resolved individually unless they bind in the highly sensitive regions. Therefore, the surroundings must be perfectly passive and the molecules efficiently guided to the nanoparticle if the sensor should be useful in applications where the sample solution truly only contain a few target molecules [110]. Further, it can be argued that this is a very rare scenario unless the content of single cells should be analyzed [111]. In most samples of interest for biosensors, the number of molecules available is very high, even for what is normally considered low concentrations. This means that the challenge normally lies in detecting a low surface coverage rather than a low number of molecules and a high degree of sensor miniaturization tends to

result in a worse detection limit in terms of surface coverage [111, 112]. However, the field has reached a state today which means that one can envision a device composed of an array of nanoplasmonic sensors that are imaged individually and in parallel, each of which capable of resolving single protein binding events. If the total number of nanoplasmonic particles is sufficiently large, the lowest detectable coverage could be extremely low, thus offering competitive limits of detection. One significant benefit of such a system is that one can envision, in analogy with single-molecule fluorescence imaging [113], that kinetic rate constants can be extracted at equilibrium binding conditions, i.e., without careful control of liquid injection and rinsing. This is possible because binding and dissociation rate constants can be obtained from the number of new binding events per time unit and the residence time of each binding event, respectively. With high time resolution, one would also be able to extract this type of information for weakly interacting components present at low concentrations, as also verified using fluorescence imaging [114].

5.2 Site-specific surface chemistry on nanoplasmonic sensors

In contrast to flat gold films used in conventional SPR sensors, patterned nanoplasmonic surfaces exhibit unique geometries (e.g., holes, tips, edges) and often a mixture of heterogeneous materials. This opens up some interesting options toward unique surface modification schemes that can enhance the utility of nanoplasmonic devices. Because refractometric sensors probe their immediate local refractive index irrespective of the identity of the molecules, the surface of the sensor must be prudently designed to detect only molecules of interest. In other words, refractometric sensors are inherently nonselective, and the analytical performance of an otherwise highly sensitive sensor can be significantly reduced by poor surface preparation. However, this requirement is not restricted to nanoplasmonic sensors; it holds for more traditional SPR approaches as well and surface-sensitive techniques in general. Most SPR and nanoplasmonic sensors employ noble metals, such as gold and silver, therefore the use of well-established thiol (-SH) chemistry to immobilize receptors is by far the most common method. When a gold or silver film is introduced into an thiol solution, the thiol groups form covalent bonds with the metal surface and after some time a well ordered self-assembled monolayer (SAM) is formed [115]. A wide variety of thiols, with varying lengths, degrees of saturation and terminal groups are
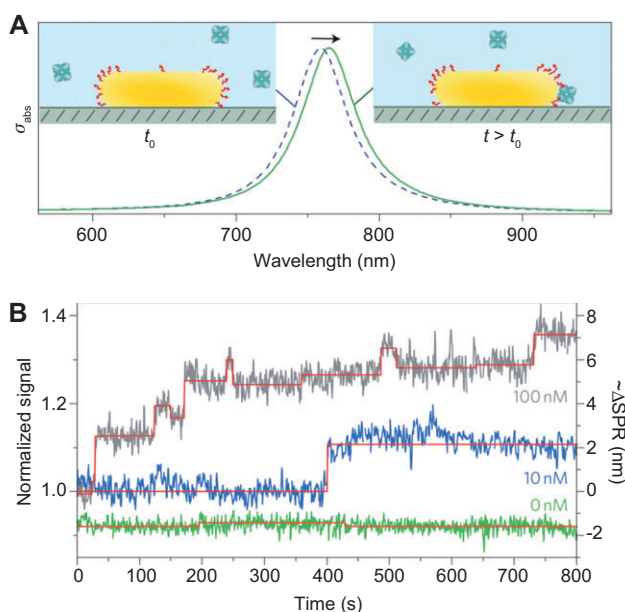
Figure 4 Binding of the analyte molecules to the receptors on a functionalized gold nanorod, shown in (A), shifts its plasmon resonance along the longitudinal direction. (B) Binding of streptavidin-R-phycoerythrin to a biotin-functionalized nanorod is monitored using photothermal microscopy. Adapted from Zijlstra et al. [108].

available commercially. Selecting a thiol with a terminal group compatible with further functionalization, such as a carboxylate or amine, allows the use of well-known conjugation schemes to immobilize proteins, peptides, small organic molecules, nucleotides and carbohydrates, preferably in plasmonically active zones.

As has been previously mentioned, plasmonic nanostructures exhibit a spatially nonuniform electromagnetic field distribution. One advantage afforded by nanoplasmonic sensors is the ability to selectively immobilize receptors at sites where the electromagnetic field is particularly strong; so-called "hot spots" such as inside nanogaps and at sharp tips and edges. In fact, when molecules bind to nanoplasmonic structures, most of the change in optical readout is due to binding at these hot spots, and the contribution to the signal change from binding elsewhere is lower. In sensing applications where equilibrium is not established, e.g., due to irreversible interactions, mass transport limitations or brief exposures to the sample solution, the sensor response can be enhanced by directing molecules to more sensitive regions.

One method to immobilize binding receptors at sensitive hot spots is through the use of thiol exchange chemistry. Beeram and Zamborini used a "place-exchange" strategy to selectively immobilize antibodies on the edges of triangular Au nanoplates, then used these functionalized nanoplates for LSPR sensing [116]. The place-exchange process takes advantage of the fact that the thiols in a SAM located on the edges of the nanoplates are more readily exchanged for thiols in solution than are thiols located on the flat surfaces of the nanoplates due to decreased steric hindrance at high-curvature sites [117].

The fabrication process for many nanoplasmonic sensors employs mixed materials, which can be exploited for site-selective surface chemistry. This is advantageous because varying material landscape leads to heterogeneous surface chemistry that can be exploited to selectively immobilize receptors at plasmonic hot spots. For example, Feuz and coworkers fabricated nanoholes in a TiO_2/Au/TiO_2 film on a glass substrate [118]. The result was a nanohole array where the top surface was coated with TiO_2, the hole sidewalls were composed of Au and the hole bottoms were coated with TiO_2. Because poly-l-lysine-poly(ethylene glycol) (PLL-PEG) selectively adsorbs to the TiO_2 surfaces, while thiolated PEG (HS-PEG) covalently bonds to the Au sidewalls, the functionalized nanohole arrays have heterogeneous chemical functionality. By employing a HS-PEG with a terminal biotin, it was possible to have avidin selectively bind to the hole sidewalls. In this sensing configuration the signal change per unit time for avidin to biotin was increased nearly

20-fold. Feuz and coworkers further showed that by using mixed materials to fabricate nanodisk pairs on a surface, they were able to direct binding of analytes to the region between the two nanodisks. This increased the signal per molecule bound by about a factor of 4 compared to binding on a single nanodisk [110]. A similar, although not as robust, approach for selective blocking and functionalization in nanoholes was presented by Ferreira et al. [119]. Since new plasmonic architectures and fabrication methods using combinations of materials are constantly being developed, the use of site-selective chemistries to boost sensor performance seems promising for certain applications [120].
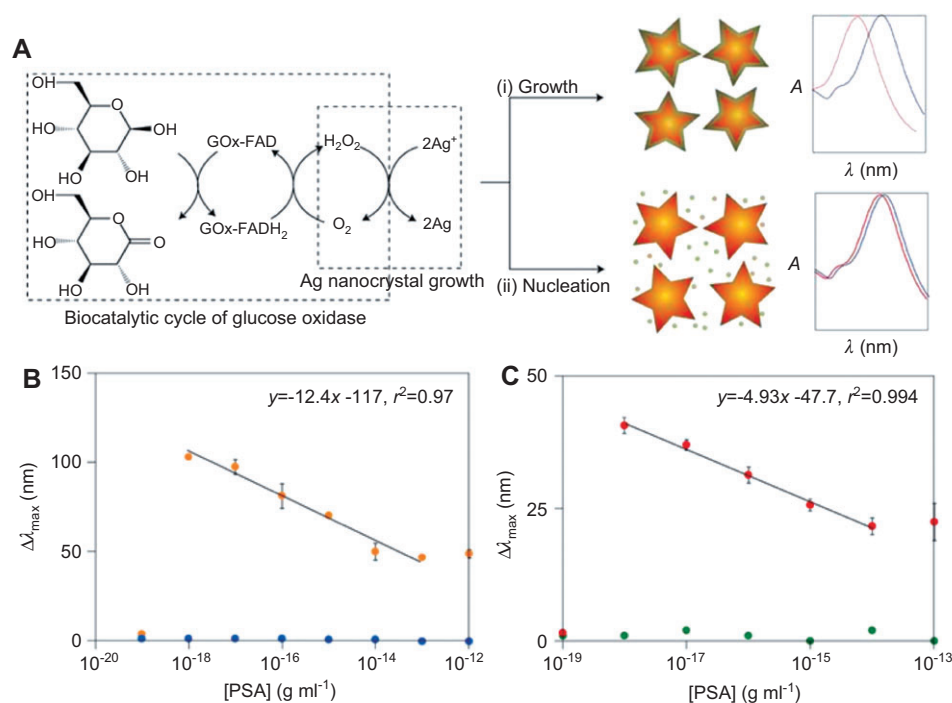
5.3 Enzyme-linked nanoplasmonic sensing

Enzymes are biological macromolecules (proteins) that function as catalysts in a wide variety of life-sustaining biochemical reactions. They also are used to amplify signals in a number of biochemical assays. Recently, groups have been harnessing the catalytic activity of enzymes to amplify the signals obtained from nanoplasmonic sensors with excellent results. In one example by Chen et al., circular Au nanodisks were fabricated on glass substrates by hole mask colloidal lithography [107]. Then the nanodisks were functionalized with a biotin-terminated SAM. Then a streptavidin-conjugated enzyme (horseradish peroxidase, HRP) in various amounts was linked to the nanodisks. Then, in the presence of H_2O_2, HRP initiated the oxidation then precipitation of 3′-3-diaminobenzidine (DAB) in its polymerized form. The polymer film deposited on the nanodisks resulted in a red-shift of the LSPR spectrum. By lowering the concentration to the pM range one or at most a few HRP molecules were immobilized on each nanodisk. These single HRP molecules were then used to catalyze the precipitation of DAB polymer on the nanodisks, which resulted in a ~3 nm shift in the single particle LSPR spectrum. These results suggest that this method could push limits of detection toward the single molecule level for clinically-relevant biochemical assays.

The vast majority of sensing schemes rely on a larger signal corresponding to the presence of a higher concentration or larger amount of analyte. Using enzyme-coupled plasmonics however, Rodriguez-Lorenzo et al. have reversed this paradigm with an inverse sensitivity readout mode, where lower analyte concentrations lead to larger signals [121]. In this work Au nanostars in solution function as the plasmonic sensing elements. An enzyme, glucose oxidase (GOx), was covalently linked to the nanostar surface, then upon addition of glucose,

H_2O_2 was generated at the nanostar surface as a byproduct of glucose oxidation. Next Ag ions were introduced into solution, and H_2O_2 reduced the Ag ions, resulting in Ag deposition on the Au nanostars. (Figure 5) When a small amount of GOx was present on the nanostars the Ag reduction pathway led to epitaxial deposition of a Ag layer on the nanostar surface, which resulted in a large blue-shift of the LSPR spectrum. But, when GOx was present in large amounts, the Ag reduction pathway favored nucleated deposition of Ag, which resulted in a much smaller spectral blue-shift. In short, less GOx on the nanostar surface results in a large change in the signal, while more GOx on the surface results in a small signal change, i.e., the calibration curve had a negative slope. This detection scheme was used to detect prostate-specific antigen (PSA), a biomarker for prostate cancer, with a sandwich immunoassay. Briefly, antibodies against PSA were immobilized on the nanostars then PSA was introduced. The anti-PSA antibodies captured the PSA, then a GOx-conjugated secondary antibody was introduced which bound to the captured PSA. The amount of GOx-conjugated antibody on the nanostars is directly proportional to the amount of captured PSA. When Ag ions were subsequently added, Ag was reduced and deposited epitaxially on the nanostars, in the case of low PSA concentrations, leading to large spectral shifts. At high PSA concentrations nucleated growth of Ag was observed, resulting in much smaller spectral shifts. The spectral shifts were linear as a function of PSA concentration between 10^{-18} and 10^{-13} g/ml, with the limit of detection being 10^{-18} g/ml. This represents an improvement of an order of magnitude over other advanced immunoassays for PSA. Because GOx can be conjugated to a wide variety of antibodies via well-known chemistries, this detection method is broadly applicable to many analytes. Moreover, the inverse sensitivity feature of this method is only possible due to the use of plasmonic nanostructures. These two examples of enzyme-linked plasmonic sensing have not shown real-time detection capabilities. However, their extreme sensitivity makes up for this shortcoming, at least when it is not critical to determine binding rate constants.

Figure 5 Inverse sensitivity sensing with enzyme-linked Au nanostars. (A) GOx generates hydrogen peroxide, which reduces silver ions to grow a silver coating around plasmonic nanosensors (Au nanostars); (i) at low concentrations of GOx the nucleation rate is slow, which favors the growth of a conformal silver coating that induces a large blueshift in the LSPR of the nanosensors; (ii) when GOx is present at high concentrations, the fast crystal growth conditions stimulate the nucleation of silver nanocrystals and less silver is deposited on the nanosensors, therefore generating a smaller variation of the LSPR. When the concentration of GOx is related to the concentration of a target molecule through immunoassay, this signal-generation step induces inverse sensitivity because condition (i) is fulfilled at low concentrations of analyte. (B, C) Blue shift of the LSPR absorbance band ($\Delta\lambda_{max}$) as a function of the concentration of PSA (orange) and BSA (blue) in buffer (B) and of PSA (red) and BSA (green) spiked into whole serum (C). Reprinted with permission from ref. [121]. Copyright 2012 Nature Publishing Group.

5.4 Combining plasmonic nanostructures with lipid bilayer membranes

Lipid bilayer membranes are found throughout nature. They comprise the membranes that define the boundaries of cells and subcellular organelles. Their primary constituents are phospholipids, which are amphiphiles that self-assemble into ~3 nm-thick bilayer structures in the presence of aqueous solutions. Embedded in natural lipid bilayer membranes are many of the proteins that are necessary for normal cell function, such as receptors, transporters and ion channels. These membranes are also decorated with a wide variety of carbohydrates. Lipid membranes are of interest to the sensing community because of their importance in the drug development process. In fact, well over half of the top 100 selling pharmaceuticals target proteins that reside on or embedded in lipid membranes [122]. Therefore, sensors that can successfully detect binding events on the surface of a lipid membrane are highly desirable. Schemes employing surface-sensitive fluorescence detection, such as total internal reflection fluorescence (TIRF) can be used [123], but they require the use of a fluorescent tag on the molecules of interest. Using a label-free detection method can eliminate the need to conjugate a fluorophore to the analyte of interest, thus plasmonic sensors are well suited to detecting molecular binding on lipid bilayer membrane.

Because natural cell membranes are difficult, though not impossible [124], to interface with plasmonic sensors, it is often convenient to use a model membrane system, such as liposomes or supported lipid bilayers (SLBs). Liposomes (also known as vesicles) are spherical lipid bilayers that can range from tens to hundreds of nanometers in diameter, while SLBs are planar lipid bilayers that are formed directly on a sensor surface and can be thought of as a 2-dimensional fluid because the lipids randomly diffuse in the SLB plane. Commercial SPR sensing systems employ specialized surface immobilization strategies to link liposomes to the surface of the sensor chip [122], even enabling sensing of membrane transport kinetics [125]. An alternative strategy, though not generally commercially available, is to alter the surface of a sensor chip such that liposomes will rupture on the surface to form a planar SLB. This can be done by coating a thin (<20 nm) layer of SiO_2 over the metallic substrate [126], with the thinnest oxide layers typically deposited by atomic layer deposition [127]. It should be noted, however, that addition of a thin oxide layer will shift the resonances of the sensor, so this must be taken into account in the sensor design process. Alternative strategies to form SLBs include

the use of thiolated lipids to covalently tether the membrane to a bare metal film, or to form SLBs on a polymer cushion which lies upon the metal film [122]. Plasmonic nanostructures can also be embedded in SLBs [128], or SLBs can be formed to envelop nanostructures, as will be discussed below. Figure 6 shows schematic illustrations of methods for interfacing membranes with plasmonic nanostructures.

One of the first examples of combining SLBs with nanoplasmonics was shown by Dahlin et al. In this work they fabricated random 110 nm-diameter holes in a Au film by colloidal lithography on a SiO_2 coated substrate [65]. The gold surface was then passivated, leaving the vesicles free to settle and rupture on the SiO_2-coated nanohole bottoms, forming SLB patches containing lipid-conjugated biotin or single-stranded DNA or the lipid receptor GM1. With this setup the introduction of cholera toxin, a 56 kDa protein which binds to GM1, induced a large increase in the extinction of the nanohole array, which was monitored as a function of time. To demonstrate that this sensing approach worked for smaller molecules as well, they were able to detect the binding of a 15-base single-stranded DNA (5 kDa) to its complementary strand that was immobilized in the SLB patches. Single vesicles can also be immobilized inside nanoholes by tagging vesicles with single-stranded DNA, then functionalizing the bottom of nanoholes with the complementary sequence [129]. Since the initial work by Dahlin et al., there have been a number of other examples where nanoholes are used to detect binding of a variety of different analytes to lipid bilayer membranes.

A challenge for combining SLBs that contain embedded proteins is that the presence of an underlying substrate can have negative effects on the protein, such as hindered diffusion and denaturation. One way to circumvent these effects is to partially remove the substrate, creating free-standing nanohole arrays that are surrounded on both sides by liquid. This allows the formation of a pore-spanning lipid membrane (PSLM) that reduces the influence of the underlying substrate on the lipids and proteins that comprise the membrane. PSLMs have been demonstrated on a variety of materials [131, 132] and been used for electrical biosensing studies [133], but examples where plasmonic sensing is used in conjunction with PSLMs are limited. In one example, Oh and coworkers formed PSLMs over SiO_2-coated Au nanoholes [127]. This allowed the insertion of a transmembrane protein, alpha-hemolysin, into the pore-spanning regions. The insertion process of the protein was followed by monitoring the transmission spectra in real-time. After protein insertion, it was possible to detect antibodies binding to alpha-hemolysin and
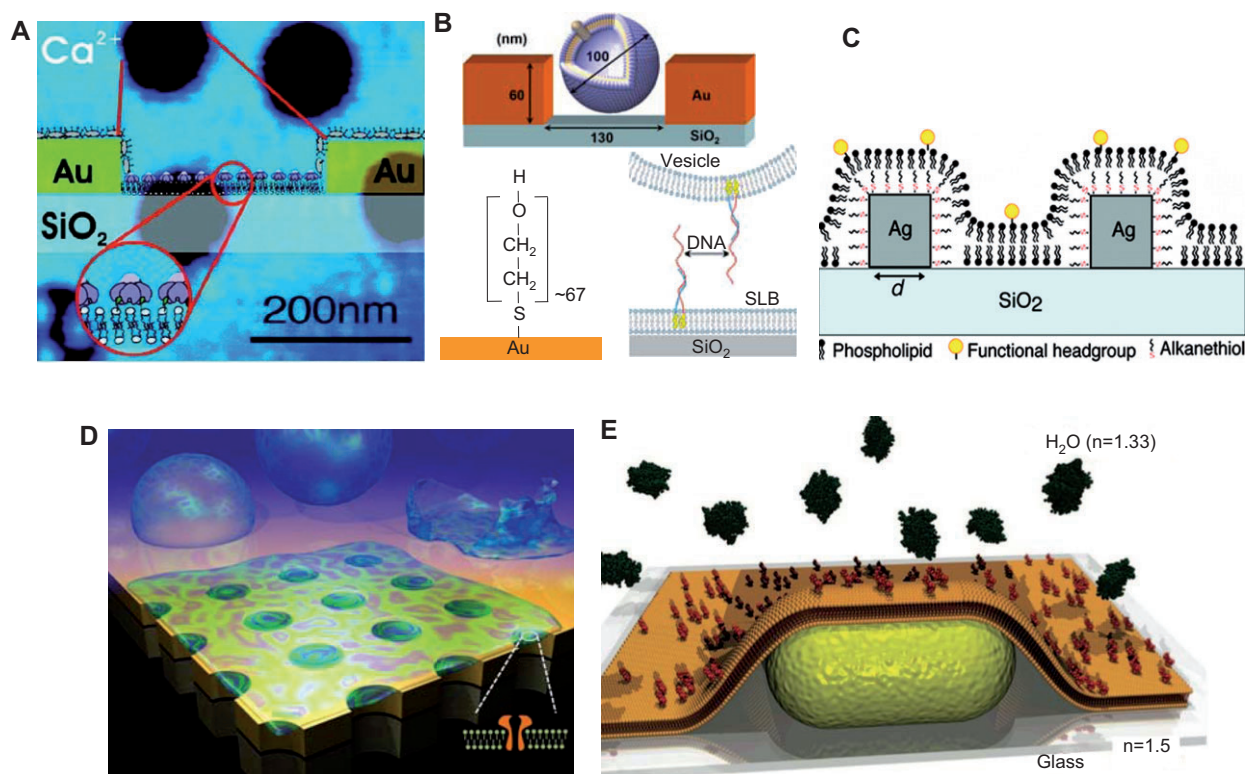
Figure 6   Integration of lipid bilayer membranes with plasmonic nanostructures. (A) Supported lipid bilayers formed on the SiO$_2$ surface at the base of Au nanoholes. From Dahlin et al. [65]. (B) Intact vesicles tethered to SiO$_2$ inside Au nanoholes via hybridization of complimentary DNA strands. From Dahlin et al. [129]. (C) Lipid bilayers formed over Ag nanocubes. The SAM on the nanocubes leads to a hybrid SAM-lipid bilayer that covers the nanocubes, while a lipid bilayer is formed on the glass between nanocubes. Adapted from Galush et al. [130]. (D) A lipid bilayer membrane suspended over nanopores in a free-standing Au film coated with an SiO$_2$ shell. Adapted from Im et al. [127]. (E) A lipid bilayer membrane decorated with proteins covering a Au nanorod. Adapted from Baciu et al. [23].

calculate binding parameters, such as association and dissociation rate constants, as well as the dissociation constant.

Instead of nanoholes, surface immobilized nanoparticles can also be combined with lipid bilayer membranes. In one example, Galush et al. deposited Ag nanocubes on a glass surface then formed a SLB over them [130]. By operating in transmission mode and monitoring the shift in the extinction maximum, binding of neutravidin to biotinylated lipids was characterized. This sensor was also used to observe unbinding of proteins from a specially functionalized lipid surface. SLB-covered Au nanorods have also been employed for lipid-protein binding assays [23]. An alternative to completely covering nanostructures is to form a SLB around them, such as the work by Lohmuller and coworkers where SLBs were formed around bow tie nanoantennas [134]. The large electromagnetic field between the antenna tips enhanced fluorescence emission, which allowed observation of individual molecules associated with the fluid 2-dimensional surface of the SLB diffusing through the tips.

5.5 Flow-through nanoplasmonic sensing

Mass transport limitations can plague all types of surface-based sensors. In order to record proper binding kinetics, an analyte must be delivered to the sensor surface at a rate that overcomes depletion at the surface due to binding. This is typically accomplished by optimizing the injection flow rate to a point where increasing flow rate does not increase the association rate constant. Unfortunately, when the sensor size shrinks, increasing the flow rate has diminishing return on improving the analyte delivery [112, 135]. Another way to overcome mass transport limitations is to force an analyte solution toward the active sensor surface. This can be achieved by using plasmonic nanoholes as nanofluidic channels.

These sensors generally rely upon free-standing open-ended nanoholes sandwiched between two microfluidic channels. In this configuration, solution approaches the nanoholes via a dead-ended microfluidic channel and then is forced through the nanoholes, where it then exits the sensing zone through a second outlet microfluidic

channel (Figure 7). By forcing liquid through nanoholes, the rate of adsorption of molecules to the surface can be increased significantly compared to the case where solution simply flows over an array of dead-ended nanoholes [136–138].

Flow-through plasmonic sensors are typically composed of a metallic layer supported by a thin film of silicon nitride, therefore it is possible to take advantage of the mixed materials to use material-specific chemistry to selectively functionalize only certain features of the nanoholes. In one example a suspended nanohole array composed of a Au layer on a Si_3N_4 thin film was functionalized with a biotinylated thiol, which is selectively immobilized on Au. Then the Si_3N_4 layer was passivated with a PEG layer [137]. This results in the binding receptors for neutravidin being localized only to the Au surface residing inside the nanoholes. Although binding occurred also on the planar part of the gold film, which also possesses

some sensitivity, the sensor response was a factor of 10 faster in the flow-through configuration than under conditions where mass transport is diffusion-limited. This means that capture-limited binding can be achieved at significantly lower flow rates, which drastically reduces sample consumption compared to standard SPR instruments. To avoid influence on the signal of biomolecular binding reactions on the less sensitive part of the gold film, Mazzotta et al. recently developed a fabrication protocol allowing discrete nanoplasmonic elements to be positioned inside the pores, thus being placed where the flow geometry is optimized for efficient binding [139].

As these examples show, pressure-driven flow through nanoholes can effectively overcome mass transport deficiencies that are associated with SPR sensing. Combining an electrophoretic concentration mechanism with a flow-though sensor architecture can further improve concentration of analytes at plasmonic nanoholes [140]. It should
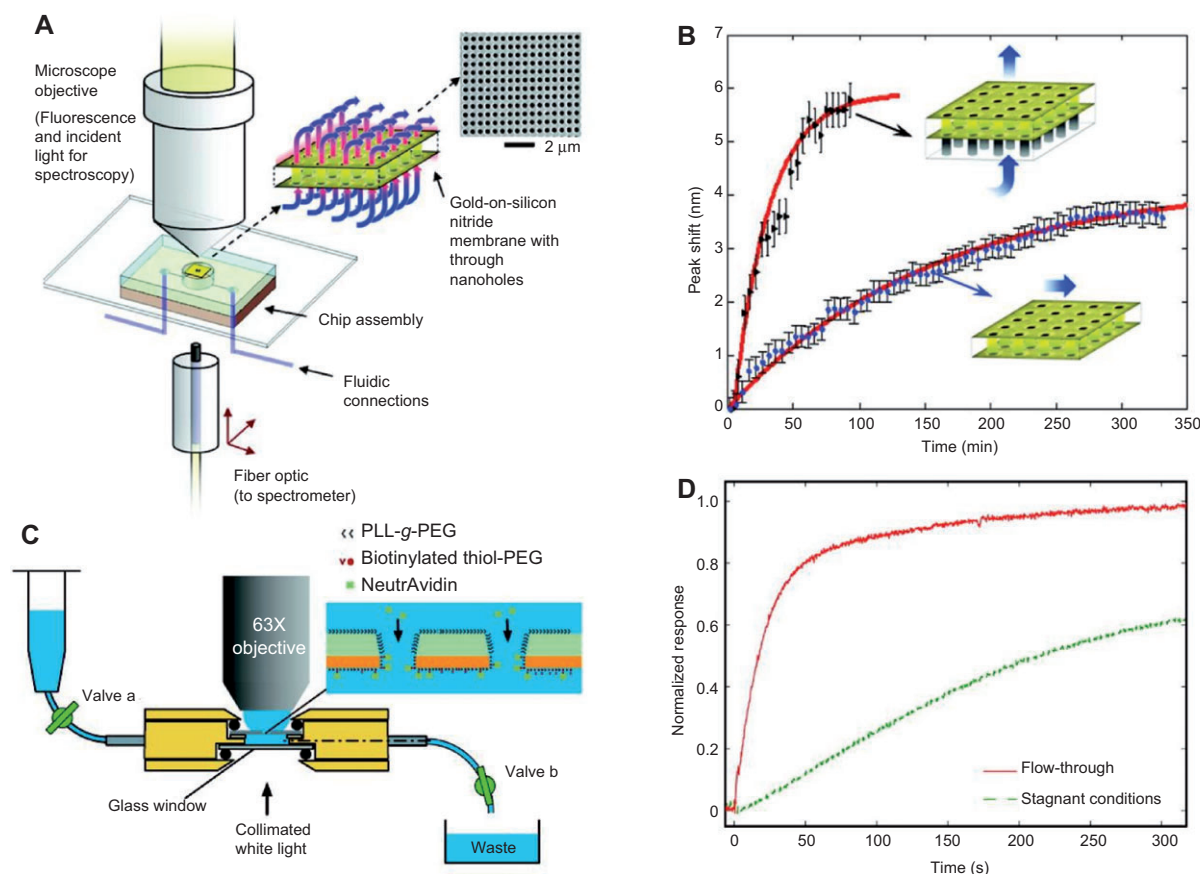
Figure 7 Flow-through nanoplasmonic sensing. (A, C) Schematic illustrations of experimental set-ups for flow-through sensing. (B) Kinetic curves showing SAM formation on a gold nanohole array in the flow-through configuration compared to the same SAM being formed using a flow-over configuration. (D) Comparison of avidin-biotin binding reactions carried out in stagnant solution vs. binding under flow-through conditions showing the drastically increased sensor response with flow-through sensing. Image A and B from Eftekhari et al. [136]; C and D from Jonsson et al. [137].

be noted that care must be exercised when applying pressure to drive the flow through nanoholes. The Si_3N_4 membrane that supports the metallic nanoholes is usually only a few hundred nanometers thick and quite delicate. Application of excessive pressure can rupture the membrane rendering the sensor useless and the experiment failed. Despite this drawback, the advantages gained by using this design make flow-through sensors a worthwhile option when sample volume limitations hinder the use of flow-over nanoplasmonic sensors or traditional SPR sensors. Recent work by Kumar et al. demonstrated that open-ended nanohole arrays have an intrinsic ability to promote flow through them via capillary flow and evaporation, which was utilized for flow-through sensing and particle assembly [141].

6 Conclusion

We have summarized the brief history and operating principles of SPR and nanoplasmonic sensors, and presented various metrics on how to evaluate the sensor performance. SPR still dominates in terms of low detection limits in surface coverage (e.g., Biacore instrument can detect ~0.01 ng/cm^2), but we have shown some examples of recent nanoplasmonic sensors that truly can go where SPR cannot. The field of nanoplasmonic biosensing has been among the most multi-disciplinary research areas: The underlying physical principles of SPR and nanoplasmonic interactions have been seamlessly integrated with state-of-the-art nanofabrication, optical instrumentation techniques, a wide range of chemical surface modification techniques, microfluidics (and now toward nanofluidic "flow-through" schemes), and biological interfacing schemes involving soft matter and cellular membranes. There is still a barrier to commercial success of nanoplasmonic devices, but increasing demand for more advanced sensors will continue to motivate researchers to overcome those hurdles.

References

[1] Dahlin AB. Plasmonic biosensors: an integrated view of refractometric detection. Washington, DC: IOS Press; 2012.

[2] Freestone I, Meeks N, Sax M, Higgitt C. The lycurgus cup – a Roman nanotechnology. Gold Bull 2007;40:270–7.

[3] Bobin O, Schvoerer M, Miane JL, Fabre JF. Coloured metallic shine associated to lustre decoration of glazed ceramics: a theoretical analysis of the optical properties. J Non-Cryst Solids 2003;332:28–34.

[4] Brown CL, Bushell G, Whitehouse MW, Agrawal DS, Tupe SG, Paknikar KM, Tiekink ERT. Nanogoldpharmaceutics. Gold Bull 2007;40:245–50.

[5] Giljohann DA, Seferos DS, Daniel WL, Massich MD, Patel PC, Mirkin CA. Gold nanoparticles for biology and medicine. Angew Chem Int Ed 2010;49:3280–94.

[6] Schultz DA. Plasmon resonant particles for biological detection. Curr Opin Biotech 2003;14:13–22.

[7] Mie G. Beiträge zur Optik trüber Medien, speziell kolloidaler Metallösungen. Annalen der Physik 1908;330:377–445.

[8] Gans R, Happel H. Zur Optik kolloidaler Metallösungen. Annalen der Physik 1909;334:277–300.

[9] Myroshnychenko V, Rodriguez-Fernandez J, Pastoriza-Santos I, Funston AM, Novo C, Mulvaney P, Liz-Marzan LM, Garcia de Abajo FJ. Modelling the optical response of gold nanoparticles. Chem Soc Rev 2008;37:1792–805.

[10] Jackson JD. Classical electrodynamics. 3rd edition. Wiley, 1998.

[11] Bohren CF, Huffman DR. Absorption and scattering of light by small particles. New York: Wiley; 1983.

[12] Kelly KL, Coronado E, Zhao LL, Schatz GC. The optical properties of metal nanoparticles: the influence of size, shape, and dielectric environment. J Phys Chem B 2003;107:668–77.

[13] Zeman EJ, Schatz GC. An accurate electromagnetic theory study of surface enhancement factors for silver, gold, copper, lithium, sodium, aluminum, gallium, indium, zinc, and cadmium. J Phys Chem 1987;91:634–43.

[14] Dahlin AB, Sannomiya T, Zahn R, Sotiriou GA, Vörös J. Electrochemical crystallization of plasmonic nanostructures. Nano Lett 2011;11:1337–43.

[15] Dahlin AB, Zahn R, Vörös J. Nanoplasmonic sensing of metal–halide complex formation and the electric double layer capacitor. Nanoscale 2012;4:2339–51.

[16] Bobbert PA, Vlieger J. The polarizability of a spheroidal particle on a substrate. Physica A 1987;147:115–41.

[17] Englebienne P. Use of colloidal gold surface plasmon resonance peak shift to infer affinity constants from the interactions between protein antigens and antibodies specific for single or multiple epitopes. Analyst 1998;123:1599–603.

[18] Nath N, Chilkoti A. A colorimetric gold nanoparticle sensor to interrogate biomolecular interactions in real time on a surface. Anal Chem 2002;74:504–9.

[19] Raschke G, Kowarik S, Franzl T, Sonnichsen C, Klar TA, Feldmann J, Nichtl A, Kurzinger K. Biomolecular recognition based on single gold nanoparticle light scattering. Nano Lett 2003;3:935–8.

[20] Nath N, Chilkoti A. Label-free biosensing by surface plasmon resonance of nanoparticles on glass: optimization of nanoparticle size. Anal Chem 2004;76:5370–8.

[21] Yu C, Irudayaraj J. Multiplex biosensor using gold nanorods. Anal Chem 2007;79:572–9.

[22] Nusz GJ, Marinakos SM, Curry AC, Dahlin AB, Höök F, Wax A, Chilkoti A. Label-free plasmonic detection of biomolecular binding by a single gold nanorod. Anal Chem 2008;80:984–9.

[23] Baciu CL, Becker J, Janshoff A, Sönnichsen C. Protein–membrane interaction probed by single plasmonic nanoparticles. Nano Lett 2008;8:1724–8.

[24] Dahlin AB, Chen S, Jonsson MP, Gunnarsson L, Käll M, Höök F. High-resolution microspectroscopy of plasmonic nanostructures for miniaturized biosensing. Anal Chem 2009;81:6572–80.

[25] Raschke G, Brogl S, Susha AS, Rogach AL, Klar TA, Feldmann J, Fieres B, Petkov N, Bein T, Nichtl A, Kurzinger K. Gold nanoshells improve single nanoparticle molecular sensors. Nano Lett 2004;4:1853–7.

[26] Haes AJ, Van Duyne RP. A nanoscale optical biosensor: sensitivity and selectivity of an approach based on the localized surface plasmon resonance spectroscopy of triangular silver nanoparticles. J Am Chem Soc 2002;124:10596–604.

[27] Larsson EM, Prinetti A, Käll M, Sutherland DS. Sensing characteristics of NIR localized surface plasmon resonances in gold nanorings for application as ultrasensitive biosensors. Nano Lett 2007;7:1256–63.

[28] Lee S, Mayer KM, Hafner JH. Improved localized surface plasmon resonance immunoassay with gold bipyramid substrates. Anal Chem 2009;81:4450–5.

[29] Dondapati SK, Sau TK, Hrelescu C, Klar TA, Stefani FD, Feldmann J. Label-free biosensing based on single gold nanostars as plasmonic transducers. ACS Nano 2010;4:6318–22.

[30] Luk'yanchuk B, Zheludev NI, Maier SA, Halas NJ, Nordlander P, Giessen H, Chong CT. The Fano resonance in plasmonic nanostructures and metamaterials. Nature Mater 2010;9:707–15.

[31] Verellen N, Van Dorpe P, Huang C, Lodewijks K, Vandenbosch GAE, Lagae L, Moshchalkov VV. Plasmon line shaping using nanocrosses for high sensitivity localized surface plasmon resonance sensing. Nano Lett 2011;11:391–7.

[32] Lange C. Berl klin Wohnschr. 1912;49:897.

[33] Green F. The colloidal gold reaction of the cerebrospinal fluid. Can Med Assoc J 1925;15:1139–43.

[34] Elghanian R. Selective colorimetric detection of polynucleotides based on the distance-dependent optical properties of gold nanoparticles. Science 1997;277:1078–81.

[35] Olofsson L, Rindzevicius T, Pfeiffer I, Käll M, Höök F. Surface-based gold-nanoparticle sensor for specific and quantitative DNA hybridization detection. Langmuir 2003;19:10414–9.

[36] Lahav M, Vaskevich A, Rubinstein I. Biological sensing using transmission surface plasmon resonance spectroscopy. Langmuir 2004;20:7365–7.

[37] Ritchie R. Plasma losses by fast electrons in thin films. Phys Rev 1957;106:874.

[38] Powell C, Swan J. Origin of the characteristic electron energy losses in aluminum. Phys Rev 1959;115:869–75.

[39] Homola J, Yee SS, Gauglitz G. Surface plasmon resonance sensors: review. Sens Actuators, B 1999;54:3–15.

[40] Homola J. Surface plasmon resonance sensors for detection of chemical and biological species. Chem Rev 2008;108:462–93.

[41] Lindquist NC, Nagpal P, McPeak KM, Norris DJ, Oh S-H. Engineering metallic nanostructures for plasmonics and nanophotonics. Rep Prog Phys 2012;75:036501.

[42] Liedberg B, Nylander C, Lundstrom I. Surface plasmon resonance for gas detection and biosensing. Sens Actuators 1983;4:299–304.

[43] Rich RL, Myszka DG. Survey of the 2009 commercial optical biosensor literature. J Mol Recognit 2011;24:892–914.

[44] Li Y-C, Chang Y-F, Su L-C, Chou C. Differential-phase surface plasmon resonance biosensor. Anal Chem 2008;80:5590–5.

[45] Zhou W-J, Halpern AR, Seefeld TH, Corn RM. Near infrared surface plasmon resonance phase imaging and nanoparticle-enhanced surface plasmon resonance phase imaging for ultrasensitive protein and DNA biosensing with oligonucleotide and aptamer microarrays. Anal Chem 2012;84:440–5.

[46] Wark AW, Lee HJ, Corn RM. Long-range surface plasmon resonance imaging for bioaffinity sensors. Anal Chem 2005;77:3904–7.

[47] Slavík R, Homola J. Ultrahigh resolution long range surface plasmon-based sensor. Sens Actuators, B 2007;123:10–2.

[48] Gordon R, Sinton D, Kavanagh KL, Brolo AG. A new generation of sensors based on extraordinary optical transmission. Acc Chem Res 2008;41:1049–57.

[49] Jonsson MP, Dahlin AB, Jönsson P, Höök F. Nanoplasmonic biosensing with focus on short-range ordered nanoholes in thin metal films (Review). Biointerphases 2008;3:FD30–FD40.

[50] Masson JF, Murray-Methot M-P, Live LS. Nanohole arrays in chemical analysis: manufacturing methods and applications. Analyst 2010;135:1483–9.

[51] Bethe HA. Theory of diffraction by small holes. Phys Rev 1944;66:163–82.

[52] Degiron A, Lezec HJ, Yamamoto N, Ebbesen TW. Optical transmission properties of a single subwavelength aperture in a real metal. Opt Commun 2004;239:61–6.

[53] Ebbesen TW, Lezec HJ, Ghaemi HF, Thio T, Wolff P. Extraordinary optical transmission through sub-wavelength hole arrays. Nature 1998;391:667–9.

[54] Przybilla F, Genet C, Ebbesen TW. Long vs short-range orders in random subwavelength hole arrays. Opt Express 2012;20:4697–709.

[55] Sannomiya T, Scholder O, Jefimovs K, Hafner C, Dahlin AB. Investigation of plasmon resonances in metal films with nanohole arrays for biosensing applications. Small 2011;7:1653–63.

[56] Pacifici D, Lezec HJ, Sweatlock LA, Walters RJ, Atwater HA. Universal optical transmission features in periodic and quasiperiodic hole arrays. Opt. Express 2008;16:9222–38.

[57] Park T-H, Mirin N, Lassiter JB, Nehl CL, Halas NJ, Nordlander P. Optical properties of a nanosized hole in a thin metallic film. ACS Nano 2008;2:25–32.

[58] Barnes WL, Dereux A, Ebbesen TW. Surface plasmon subwavelength optics. Nature 2003;424:824–30.

[59] Genet C, Ebbesen TW. Light in tiny holes. Nature 2007;445:39–46.

[60] de Ajajo FJG. Colloquium: Light scattering by particle and hole arrays. Rev Mod Phys 2007;79:1267.

[61] García-Vidal FJ, Ebbesen TW, Kuipers L. Light passing through subwavelength apertures. Rev Mod Phys 2010;82:729–87.

[62] Genet C, Van Exter MP, Woerdman J. Fano-type interpretation of red shifts and red tails in hole array transmission spectra. Opt Commun 2003;225:331–6.

[63] Braun J, Gompf B, Kobiela G, Dressel M. How holes can obscure the view: suppressed transmission through an ultrathin

metal film by a subwavelength hole array. Phys Rev Lett 2009;103:203901.

[64] Brolo AG, Gordon R, Leathem B, Kavanagh KL. Surface plasmon sensor based on the enhanced light transmission through arrays of nanoholes in gold films. Langmuir 2004;20: 4813–5.

[65] Dahlin AB, Zäch M, Rindzevicius T, Käll M, Sutherland DS, Höök F. Localized surface plasmon resonance sensing of lipid-membrane-mediated biorecognition events. J Am Chem Soc 2005;127:5043–8.

[66] Rindzevicius T, Alaverdyan Y, Dahlin AB, Höök F, Sutherland DS, Käll M. Plasmonic sensing characteristics of single nanometric holes. Nano Lett 2005;5:2335–9.

[67] Laromaine A, Koh L, Murugesan M, Ulijn RV, Stevens MM. Protease-triggered dispersion of nanoparticle assemblies. J Am Chem Soc 2007;129:4156–7.

[68] Lodewijks K, Van Roy W, Borghs G, Lagae L, Van Dorpe P. Boosting the figure-of-merit of lspr-based refractive index sensing by phase-sensitive measurements. Nano Lett 2012;12:1655–9.

[69] Dahlin AB, Tegenfeldt JO, Höök F. Improving the instrumental resolution of sensors based on localized surface plasmon resonance. Anal Chem 2006;78:4416–23.

[70] Murray-Methot M-P, Ratel M, Masson J-F. Optical properties of Au, Ag, and bimetallic Au on Ag nanohole arrays. J Phys Chem C 2010;114:8268–75.

[71] Piliarik M, Homola J. Surface plasmon resonance (SPR) sensors: approaching their limits? Opt Express 2009;17:16505–17.

[72] Dahlin AB, Jonsson MP. Nanoplasmonic sensors. In: Dmitriev A, editor. New York, NY: Springer; 2012, pp. 231–65.

[73] Becker J, Trügler A, Jakab A, Hohenester U, Sönnichsen C. The optimal aspect ratio of gold nanorods for plasmonic bio-sensing. Plasmonics 2010;5:161–7.

[74] Das M, Hohertz D, Nirwan R, Brolo AG, Kavanagh KL, Gordon R. Improved performance of nanohole surface plasmon resonance sensors by the integrated response method. IEEE Photonics J 2011;3:441–9.

[75] Svedendahl M, Chen S, Dmitriev A, Käll M. Refractometric sensing using propagating versus localized surface plasmons: a direct comparison. Nano Lett 2009;9:4428–33.

[76] Johnsson B, Löfås S, Lindquist G. Immobilization of proteins to a carboxymethyldextran-modified gold surface for biospecific interaction analysis in surface plasmon resonance sensors. Anal Biochem 1991;198:268–77.

[77] Kedem O, Tesler AB, Vaskevich A, Rubinstein I. Sensitivity and optimization of localized surface plasmon resonance transducers. ACS Nano 2011;5:748–60.

[78] Prikulis J, Hanarp P, Olofsson L, Sutherland D, Käll M. Optical spectroscopy of nanometric holes in thin gold films. Nano Lett 2004;4:1003–7.

[79] Lee SH, Bantz KC, Lindquist NC, Oh S-H, Haynes CL. Self-assembled plasmonic nanohole arrays. Langmuir 2009;25:13685–93.

[80] Tetz K, Pang L, Fainman Y. High-resolution surface plasmon resonance sensor based on linewidth-optimized nanohole array transmittance. Opt Lett 2006;31:1528–30.

[81] Henzie J, Lee MH, Odom TW. Multiscale patterning of plasmonic metamaterials. Nature Nanotech 2007;2:549–54.

[82] Menezes JW, Ferreira J, Santos MJL, Cescato L, Brolo AG. Large-area fabrication of periodic arrays of nanoholes in metal films and their application in biosensing and plasmonic-enhanced photovoltaics. Adv Funct Mater 2010;20:3918–24.

[83] Nagpal P, Lindquist NC, Oh S-H, Norris DJ. Ultrasmooth patterned metals for plasmonics and metamaterials. Science 2009;325:594–7.

[84] Im H, Lee SH, Wittenberg NJ, Johnson TW, Lindquist NC, Nagpal P, Norris DJ, Oh S-H. Template-stripped smooth ag nanohole arrays with silica shells for surface plasmon resonance biosensing. ACS Nano 2011;5:6244–53.

[85] Lindquist NC, Johnson TW, Norris DJ, Oh S-H. Monolithic integration of continuously tunable plasmonic nanostructures. Nano Lett 2011;11:3526–30.

[86] Park JH, Ambwani P, Manno M, Lindquist NC, Nagpal P, Oh S-H, Leighton C, Norris DJ. Single-crystalline silver films for plasmonics. Adv Mater 2012;24:3988–92.

[87] Piliarik M, Párová L, Homola J. High-throughput SPR sensor for food safety. Biosens Bioelectron 2009;24:1399–404.

[88] Vala M, Chadt K, Piliarik M, Homola J. High-performance compact SPR sensor for multi-analyte sensing. Sens Actuators, B 2010;148:544–9.

[89] Lindquist NC, Lesuffleur A, Im H, Oh S-H. Sub-micron resolution surface plasmon resonance imaging enabled by nanohole arrays with surrounding Bragg mirrors for enhanced sensitivity and isolation. Lab Chip 2009;9:382–7.

[90] Nakamoto K, Kurita R, Niwa O, Fujii T, Nishida M. Development of a mass-producible on-chip plasmonic nanohole array biosensor. Nanoscale 2011;3:5067–75.

[91] Nakamoto K, Kurita R, Niwa O. Electrochemical surface plasmon resonance measurement based on gold nanohole array fabricated by nanoimprinting technique. Anal Chem 2012;84:3187–91.

[92] Lindquist NC, Johnson TW, Jose J, Otto LM, Oh S-H. Ultrasmooth metallic films with buried nanostructures for backside reflection-mode plasmonic biosensing. Annalen der Physik 2012;524:687–96.

[93] Stein B, Laluet J-Y, Devaux E, Genet C, Ebbesen TW. Fano resonances and leakage radiation for high-resolution plasmonic sensing. J Phys Chem C 2012;116:6092–6.

[94] Moreira CS, Lima AMN, Neff H, Thirstrup C. Temperature-dependent sensitivity of surface plasmon resonance sensors at the gold–water interface. Sens Actuators, B 2008;134:854–62.

[95] Baffou G, Quidant R. Thermo-plasmonics: using metallic nano-structures as nano-sources of heat. Laser & Photon Rev 2012. In press.

[96] Im H, Sutherland JN, Maynard JA, Oh S-H. Nanohole-based surface plasmon resonance instruments with improved spectral resolution quantify a broad range of antibody-ligand binding kinetics. Anal Chem 2012;84:1941–7.

[97] Stewart ME, Mack NH, Malyarchuk V, Soares JANT, Lee TW, Gray SK, Nuzzo RG, Rogers JA. Quantitative multispectral biosensing and 1D imaging using quasi-3D plasmonic crystals. Proc Natl Acad Sci USA 2006;103:17143–8.

[98] Lee SH, Lindquist NC, Wittenberg NJ, Jordan LR, Oh S-H. Real-time full-spectral imaging and affinity measurements from 50 microfluidic channels using nanohole surface plasmon resonance. Lab Chip 2012;12:3882–90.

[99] Nusz GJ, Marinakos SM, Rangarajan S, Chilkoti A. Dual-order snapshot spectral imaging of plasmonic nanoparticles. Appl Opt 2011;50:4198–206.

[100] Lesuffleur A, Im H, Lindquist NC, Lim KS, Oh S-H. Laser-illuminated nanohole arrays for multiplex plasmonic microarray sensing. Opt Express 2008;16:219–24.

[101] Ji J, O'Connell JG, Carter DJD, Larson DN. High-throughput nanohole array based system to monitor multiple binding events in real time. Anal Chem 2008;80:2491–8.

[102] Yang J-C, Ji J, Hogle JM, Larson DN. Metallic nanohole arrays on fluoropolymer substrates as small label-free real-time bioprobes. Nano Lett 2008;8:2718–24.

[103] Endo T, Kerman K, Nagatani N, Hiepa HM, Kim DK, Yonezawa Y, Nakano K, Tamiya E. Multiple label-free detection of antigen–antibody reaction using localized surface plasmon resonance-based core–shell structured nanoparticle layer nanochip. Anal Chem 2006;78:6465–75.

[104] Ament I, Prasad J, Henkel A, Schmachtel S, Sönnichsen C. Single unlabeled protein detection on individual plasmonic nanoparticles. Nano Lett 2012;12:1092–5.

[105] McFarland AD, Van Duyne RP. Single silver nanoparticles as real-time optical sensors with zeptomole sensitivity. Nano Lett 2003;3:1057–62.

[106] Nusz GJ, Curry AC, Marinakos SM, Wax A, Chilkoti A. Rational selection of gold nanorod geometry for label-free plasmonic biosensors. ACS Nano 2009;3:795–806.

[107] Chen S, Svedendahl M, Van Duyne RP, Käll M. Plasmon-enhanced colorimetric ELISA with single molecule sensitivity. Nano Lett 2011;11:1826–30.

[108] Zijlstra P, Paulo PMR, Orrit M. Optical detection of single non-absorbing molecules using the surface plasmon resonance of a gold nanorod. Nature Nanotech 2012;7:379–82.

[109] Boyer D, Tamarat P, Maali A, Lounis B, Orrit M. Photothermal imaging of nanometer-sized metal particles among scatterers. Science 2002;297:1160–3.

[110] Feuz L, Jonsson MP, Höök F. Material-selective surface chemistry for nanoplasmonic sensors: optimizing sensitivity and controlling binding to local hot spots. Nano Lett 2012;12:873–9.

[111] Dahlin AB. Size matters: problems and advantages associated with highly miniaturized sensors. Sensors 2012;12:3018–36.

[112] Squires TM, Messinger RJ, Manalis SR. Making it stick: convection, reaction and diffusion in surface-based biosensors. Nat Biotechnol 2008;26:417–26.

[113] Gunnarsson A, Jönsson P, Marie R, Tegenfeldt JO, Höök F. Single-molecule detection and mismatch discrimination of unlabeled DNA targets. Nano Lett 2008;8:183–8.

[114] Bally M, Gunnarsson A, Svensson L, Larson G, Zhdanov V, Höök F. Interaction of single viruslike particles with vesicles containing glycosphingolipids. Phys Rev Lett 2011;107:188103.

[115] Love JC, Estroff LA, Kriebel JK, Nuzzo RG, Whitesides GM. Self-assembled monolayers of thiolates on metals as a form of nanotechnology. Chem Rev 2005;105:1103–70.

[116] Beeram SR, Zamborini FP. Selective attachment of antibodies to the edges of gold nanostructures for enhanced localized surface plasmon resonance biosensing. J Am Chem Soc 2009;131:11689–91.

[117] Hostetler MJ, Templeton AC, Murray RW. Dynamics of place-exchange reactions on monolayer-protected gold cluster molecules. Langmuir 1999;15:3782–9.

[118] Feuz L, Jönsson P, Jonsson MP, Höök F. Improving the limit of detection of nanoscale sensors by directed binding to high-sensitivity areas. ACS Nano 2010;4:2167–77.

[119] Ferreira J, Santos MJL, Rahman MM, Brolo AG, Gordon R, Sinton D, Girotto EM. Attomolar protein detection using in-Hole surface plasmon resonance. J Am Chem Soc 2009;131:436–7.

[120] Marie R, Dahlin AB, Tegenfeldt JO, Höök F. Generic surface modification strategy for sensing applications based on Au/SiO$_2$ nanostructures. Biointerphases 2007;2:49–55.

[121] Rodríguez-Lorenzo L, la Rica de R, Álvarez-Puebla RA, Liz-Marzan LM, Stevens MM. Plasmonic nanosensors with inverse sensitivity by means of enzyme-guided crystal growth. Nature Mater 2012;11:604–7.

[122] Cooper MA. Advances in membrane receptor screening and analysis. J Mol Recognit 2004;17:286–315.

[123] Shi J, Yang T, Kataoka S, Zhang Y, Diaz AJ, Cremer PS. GM$_1$ clustering inhibits cholera toxin binding in supported phospholipid membranes. J Am Chem Soc 2007;129:5954–61.

[124] Wittenberg NJ, Im H, Johnson TW, Xu X, Warrington AE, Rodriguez M, Oh S-H. Facile assembly of micro- and nanoarrays for sensing with natural cell membranes. ACS Nano 2011;5:7555–64.

[125] Brändén M, Dahlin S, Höök F. Label-free measurements of molecular transport across liposome membranes using evanescent-wave sensing. ChemPhysChem 2008;9:2480–5.

[126] Jonsson MP, Jönsson P, Dahlin AB, Höök F. Supported lipid bilayer formation and lipid-membrane-mediated biorecognition reactions studied with a new nanoplasmonic sensor template. Nano Lett 2007;7:3462–8.

[127] Im H, Wittenberg NJ, Lesuffleur A, Lindquist NC, Oh S-H. Membrane protein biosensing with plasmonic nanopore arrays and pore-spanning lipid membranes. Chem Sci 2010;1:688–96.

[128] Lohmüller T, Triffo S, O'Donoghue GP, Xu Q, Coyle MP, Groves JT. Supported membranes embedded with fixed arrays of gold nanoparticles. Nano Lett 2011;11:4912–8.

[129] Dahlin AB, Jonsson MP, Höök F. Specific self-assembly of single lipid vesicles in nanoplasmonic apertures in gold. Adv Mater 2008;20:1436–42.

[130] Galush WJ, Shelby SA, Mulvihill MJ, Tao A, Yang P, Groves JT. A nanocube plasmonic sensor for molecular binding on membrane surfaces. Nano Lett 2009;9:2077–82.

[131] Hennesthal C, Steinem C. Pore-spanning lipid bilayers visualized by scanning force microscopy. J Am Chem Soc 2000;122:8085–6.

[132] Lazzara TD, Carnarius C, Kocun M, Janshoff A, Steinem C. Separating attoliter-sized compartments using fluid pore-spanning lipid bilayers. ACS Nano 2011;5:6935–44.

[133] Janshoff A, Steinem C. Transport across artificial membranes–an analytical perspective. Anal Bioanal Chem 2006;385:433–51.

[134] Lohmüller T, Iversen L, Schmidt M, Rhodes C, Tu HL, Lin WC, Groves JT. Single molecule tracking on supported membranes with arrays of optical nanoantennas. Nano Lett 2012;12:1717–21.

[135] Sheehan PE, Whitman LJ. Detection limits for nanoscale biosensors. Nano Lett 2005;5:803–7.

[136] Eftekhari F, Escobedo C, Ferreira J, Duan X, Girotto EM, Brolo AG, Gordon R, Sinton D. Nanoholes as nanochannels: flow-through plasmonic sensing. Anal Chem 2009;81:4308–11.

[137] Jonsson MP, Dahlin AB, Feuz L, Petronis S, Höök F. Locally functionalized short-range ordered nanoplasmonic pores for bioanalytical sensing. Anal Chem 2010;82:2087–94.

[138] Escobedo C, Brolo AG, Gordon R, Sinton D. Flow-through vs flow-over: analysis of transport and binding in nanohole array plasmonic biosensors. Anal Chem 2010;82: 10015–20.

[139] Mazzotta F, Höök F, Jonsson MP. High throughput fabrication of plasmonic nanostructures in nanofluidic pores for biosensing applications. Nanotechnology 2012;23:415304.

[140] Escobedo C, Brolo AG, Gordon R, Sinton D. Optofluidic concentration: plasmonic nanostructure as concentrator and sensor. Nano Lett 2012;12:1592–6.

[141] Kumar S, Wittenberg NJ, Oh, S-H. Nanopore-induced spontaneous concentration for optofluidic sensing and particle assembly. Anal Chem 2012, DOI: 10.1021/ac302690w.